SEARCH FOR THE STANDARD MODEL $Higgs \rightarrow ZZ^{(*)} \rightarrow 4\,leptons$ IN ATLAS

Konstantinos Nikolopoulos
University of Athens, Athens, GR 15771, Greece
Brookhaven National Laboratory, Upton, NY 11973, USA
On behalf of the ATLAS collaboration

Abstract

The sensitivity of the ATLAS experiment to possible discovery channels has been recently re-evaluated using complete - "as built" - detector simulation, latest theoretical cross-section calculations, optimized selection criteria and appropriate statistical treatment. In this contribution, the sensitivity to $H \rightarrow ZZ^{(*)} \rightarrow 4l$, which covers the Standard Model Higgs discovery in the mass range from $\approx 120\,GeV$ to $\approx 700\,GeV$, is presented. The four lepton signature makes this channel very promising, even for the detector start-up phase, while it poses stringent requirements in terms of lepton identification and measurement capabilities.

1 Introduction

The Standard Model of electroweak and strong interactions has been proved to be in excellent agreement with the numerous experimental measurements performed over the last thirty years. However, the underlying dynamics of the electroweak symmetry breaking is still not known. Within the Standard Model, the electroweak symmetry is spontaneously broken via the Higgs mechanism. A doublet of complex scalar fields is introduced, out of which only a single neutral scalar particle, the Higgs boson, remains after symmetry breaking.

The Higgs boson is the only piece of the Standard Model lacking experimental verification. Indeed, the discovery of the Higgs boson, or the explanation of the electroweak symmetry breaking by other means, is one of the main **L**arge **H**adron **C**ollider (LHC) goals.

Although the Higgs boson mass is not predicted in the Standard Model, it can be constrained by virtue of the loop corrections to the electroweak observables. Assuming the overall validity of the Standard Model, a global fit is performed to the high precision electroweak data which leads to $m_H = 76^{+33}_{-24} GeV$, favoring a light Higgs boson with $m_H < 144\, GeV$ at 95% confidence level [1)].

On the direct searches for the Higgs boson the best lower limit $m_H > 114.4\, GeV$ at 95% confidence level comes from LEP-2 [2)]. Using this direct limit in the global electroweak fit, $m_H < 182\, GeV$ at 95% confidence level. Currently, direct searches for the Higgs boson are conducted at the Tevatron, where CDF and DØ might exclude a mass region around 160 GeV before LHC comes into play.

2 The ATLAS experiment at the LHC

The LHC is a pp accelerator installed in the pre-existing, 27 km long, LEP (**L**arge **E**lectron **P**ositron) tunnel. It will operate at $\sqrt{s} = 14 TeV$ with nominal luminosity of $L = 10^{34} cm^{-2} s^{-1}$. According to the current[1] LHC schedule, the first pilot physics run at $\sqrt{s} = 10\, TeV$ and $L \approx 10^{32} cm^{-2} s^{-1}$ will take place in 2008.

The ATLAS (**A** **T**oroidal **L**HC **A**pparatu**S**) experiment [3)] is a general-purpose detector designed to fully exploit the physics potential of the LHC by

[1]May 2008.

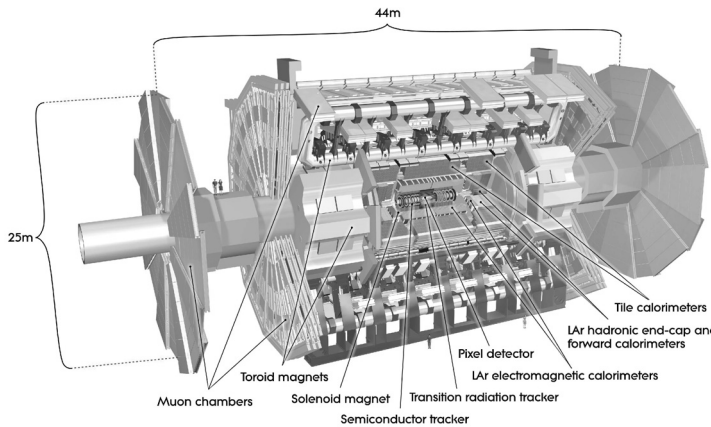

Figure 1: *Schematic view of the ATLAS detector.*

providing efficient and precise measurements of electrons, photons, muons, taus, light flavor and b-quark jets and missing transverse momentum. A schematic view of the ATLAS detector is given in Fig. 1, while its main characteristics are summarized in Table 1.

Table 1: *Main features of the ATLAS detector.*

Inner detector	Si pixels and strips Transition Radiation Tracker $2\,T$ solenoid magnetic field $\sigma_{p_T}/p_T = 0.05\% \cdot p_T \oplus 1\%$
Electromagnetic calorimeter	Pb-liquid Argon Longitudinal and lateral segmentation $\sigma_E/E \approx 10\%/\sqrt{E(GeV)} \oplus 0.7\%$
Hadronic calorimeter	Fe-scintillator + Cu-liquid Argon $\sigma_E/E \approx 50\%/\sqrt{E(GeV)} \oplus 3\%$
Muon Spectrometer	Air-core toroid magnetic field Stand-alone triggering and measurement $\sigma_{p_T}/p_T \approx 10\%$ at $p_T = 1000\,GeV$ (stand-alone) $\sigma_{p_T}/p_T \approx 2.3\%$ at $p_T = 50\,GeV$ (with inner detector)

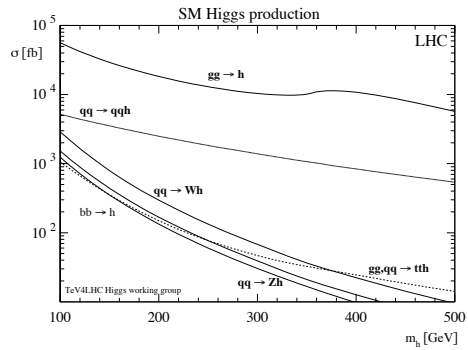

Figure 2: *Higgs boson production cross sections for the most relevant mechanisms as a function of the Higgs mass* [4].

3 Standard Model Higgs production and decay

The Higgs boson couples preferentially to the heavy particles and this determines its production mechanisms and decay modes. At the LHC the dominant production mechanism for the Standard Model Higgs boson is the gluon fusion, $gg \rightarrow H$, which at lowest order proceeds via a heavy quark loop. The vector boson fusion, $qq \rightarrow qqH$, follows with the exclusive signature of two forward quark jets and the lack of color exchange between those quarks. Other production mechanisms are the associated production with weak gauge bosons, $q\bar{q} \rightarrow WH/ZH$, and the associated production with heavy quarks, for example $gg, q\bar{q} \rightarrow t\bar{t}H$. These latter mechanisms are mainly relevant for low mass Higgs searches. The production cross-sections are summarized in Fig. 2 as a function of the Higgs mass.

The decay modes of the Standard Model Higgs as a function of its mass are summarized in Fig. 3(a). The branching ratios to WW and ZZ are dominant when kinematically accessible. The total Higgs decay width, which is negligible compared to the experimental resolution for low masses, increases rapidly and becomes significant above the ZZ production threshold, as shown in Fig. 3(b).

4 The $H \rightarrow ZZ^{(*)} \rightarrow 4l$ channel

This is a powerful and simple but yet demanding channel for discovering the Standard Model Higgs in the mass range from 120 GeV to about 700 GeV.

In the high mass region it exhibits the striking signature of two on-shell Z bosons decaying to lepton pairs, while for lower masses - due to phase space constraints - one Z boson is on-shell and the other is pushed to lower masses. Furthermore, the Z bosons decay to lepton pairs, $e^+e^-/\mu^+\mu^-$, provide a very clean signature with only electrons and muons in the final state. This is a very important aspect, especially in the initial LHC phase where the leptons will be the first objects that will be understood.

By virtue of having only electrons and muons in the final state, the event can be fully reconstructed and a narrow mass peak can be observed in most of the mass interval. Furthermore, the smooth distribution of the background below the mass peak allows for its direct estimation from data.

However, due to the relatively low cross-section and the presence of four leptons in the final state, excellent lepton detection, identification and measurement is of paramount importance. The $H \rightarrow ZZ^{(*)} \rightarrow 4l$ is a benchmark channel for the detector performance and constituted a design consideration for the ATLAS detector. In Fig. 4 the electron and muon detection efficiency is shown as a function of their transverse momentum.

The main backgrounds to this channel are the irreducible $ZZ^{(*)}/\gamma^{(*)} \rightarrow 4l$ and the reducible $Zb\bar{b} \rightarrow 4l$ and $t\bar{t} \rightarrow W^+bW^-\bar{b} \rightarrow 4l$. Other secondary backgrounds like $WZ \rightarrow 3l + fake\ lepton$ were found to be negligible. The inclusive Z boson production $Z \rightarrow 2l + X \rightarrow 4l$, with one lepton pair produced

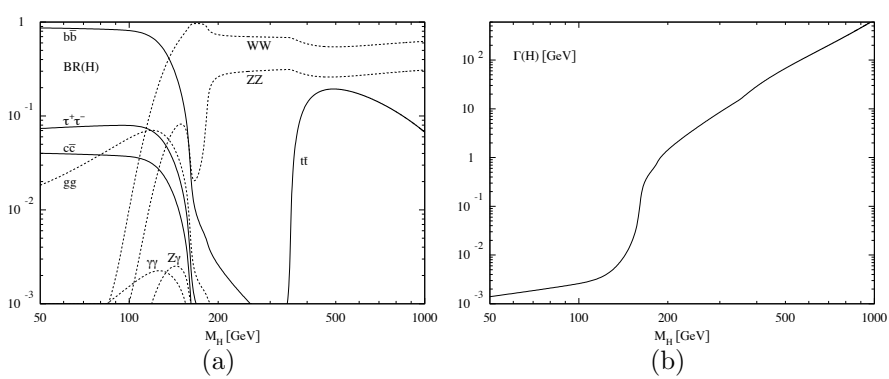

Figure 3: *The Standard Model Higgs boson decay branching fractions (a) and total width (b) as a function of the Higgs mass* [5].

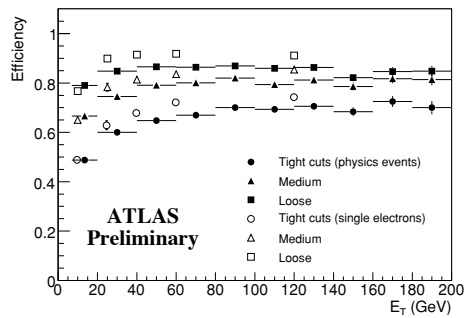

(a)

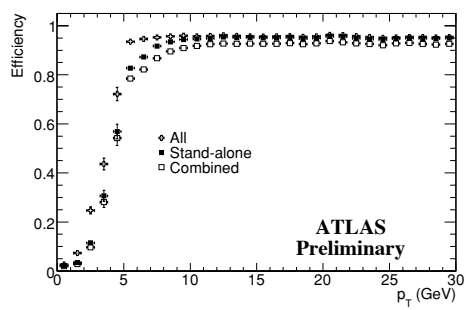

(b)

Figure 4: *The efficiency in detecting and identifying electrons (a) and muons (b) in ATLAS as a function of their transverse momentum* [6].

by the Z boson decay and the second lepton pair originating from charged hadrons misidentified as electrons, by photon conversions or by muons from meson decays, needs to be reduced well below the irreducibile background level.

5 Sensitivity study

The discovery potential of the $H \rightarrow ZZ^{(*)} \rightarrow 4l$ channel has been revisited recently. The signal and background cross-sections have been normalized to the Next-to-Leading Order calculations, including mass dependent K-factors where appropriate. Furthermore, the performance of the trigger chain has

been studied for the first time, while the effects of low luminosity pile-up[2] and cavern background[3] have been estimated. Finally, the layout of the as-built detector, including a detailed material description, has been used.

Three distinct final states can be defined: the $H \rightarrow 4\mu$ which is the cleanest with only muons present in the final state, the $H \rightarrow 4e$ and the $H \rightarrow 2e2\mu$ which has two times higher branching ratio with respect to the other two final states.

5.1 Event triggering and lepton preselection

In order to trigger the experiment on $H \rightarrow ZZ^{(*)} \rightarrow 4l$ events it is foreseen to use dilepton triggers, where the leptons are required to exceed a certain transverse momentum threshold. For the low luminosity phase high-p_T single lepton triggers are also feasible. The two approaches are equally efficient, reaching a signal trigger efficiency close to 100% for the events selected by the offline analysis.

For considering a lepton in the offline analysis it should fulfill certain quality criteria, for example concerning the shape of the electromagnetic shower associated with an electron. Then, similarly to the Physics Performance Technical Design Report analysis [3)], each candidate event should have at least four leptons passing the quality criteria in the pseudorapidity range $|\eta| < 2.5$ and $p_T > 7GeV$. Furthermore, at least two of the leptons should exceed the high-p_T threshold of $20\,GeV$ as well.

The selected leptons of the event are used to form two same flavor but opposite sign dilepton candidates. Each event is required to have a dilepton with invariant mass consistent with the Z boson mass, $|M_{l^+l^-} - M_Z| < 15\,GeV$ for $m_H = 130\,GeV$, in order to suppress non-resonant backgrounds like $t\bar{t}$. The second dilepton is required to have a mass higher than a threshold, $M_{l^+l^-} > 20\,GeV$ for $m_H = 130\,GeV$, which eventually evolves in requiring two on-shell dileptons in searches at the high mass region.

[2]At "low luminosity" the instantaneous luminosity is $10^{33}cm^{-2}s^{-1}$ and there are ≈ 2.3 interactions per bunch crossing.

[3]Spurious hits due to photons and thermal neutrons produced in the shielding material and machine elements.

5.2 Rejection of reducible backgrounds

To further reject the reducible backgrounds, the topology difference with the signal, which is the presence of two b-jets in the final state, can be exploited. In this case, the semileptonic decays of b and c quarks result in non-isolated leptons from displaced vertices.

5.2.1 Isolation

The calorimeter isolation is defined as the sum of the transverse energy deposited in the calorimeter inside a cone of radius $\Delta R = \sqrt{\Delta\eta^2 + \Delta\phi^2}$, in the pseudorapidity-azimuthal angle space, around the lepton. The energy deposition of the lepton itself is subtracted from the isolation energy. The isolation energy of the less isolated lepton is used as the discriminating variable.

Correspondingly, the track isolation is defined as the sum of the transverse momentum of the inner detector tracks in a cone of radius ΔR, around the lepton. The tracks of the four leptons forming the two dilepton pairs are excluded from the sum. The maximum track isolation energy of all leptons in the event is used as the discriminant

A cone size of 0.2 represents a good compromise between the jet physics, which requires a large cone, and the event pile-up, requiring small cone size. The background rejection, especially in the case of $Zb\bar{b}$, improves substantially when the isolation energy is normalized to the transverse momentum of the lepton under examination.

In Fig. 5 the distributions of normalized calorimeter and track isolation for the Higgs signal, $m_H = 130\,GeV$, and the two main reducible backgrounds are presented for the 4μ channel. The difference between the signal and the backgrounds is evident.

5.2.2 Impact parameter

Leptons from $t\bar{t}$ and $Zb\bar{b}$ backgrounds are most likely to originate from displaced vertices. This characteristic can be exploited by using the transverse impact parameter significance of the leptons, which is defined as the ratio of the transverse impact parameter over its measurement error. The impact parameter is measured with respect to the primary vertex of the event, the latter being estimated from a set of tracks reconstructed in the Inner Detector. This

accounts for the spread of the vertex position, which at LHC is 15 μm on the transverse plane and $\approx 55\, mm$ along the beam axis. In the case of electrons, bremsstrahlung affects the impact parameter distribution, hence reducing the discriminating power of this variable with respect to muons.

In Fig. 6, the maximum normalized transverse impact parameter significance for signal, $m_H = 130\, GeV$, and the main reducible backgrounds in the 4μ channel is shown.

5.3 Mass reconstruction

As presented in Fig. 3(b), for Higgs masses larger than $\approx 230\, GeV$ the Higgs natural width dominates over the detector resolution. On the other hand, for lower Higgs masses the Higgs natural width is negligible and the mass resolution becomes crucial for discovery. To further improve the mass resolution a Z mass constraint is applied to the on-shell Z boson, taking into account the natural Z width. In Fig. 7 the Higgs mass resolution in the 4μ channel is presented before and after the application of the Z mass constraint demonstrating a 10% improvement in the Higgs mass resolution for $m_H = 130\, GeV$.

5.4 Mass distributions and expected significance

Using the isolation and impact parameter criteria a further rejection of $O(10^2)$ for $Zb\bar{b}$ and $O(10^3)$ for $t\bar{t}$ is achieved for a signal efficiency of $O(80\%)$. The effect of the low luminosity pile-up was estimated to be less than 5%. The

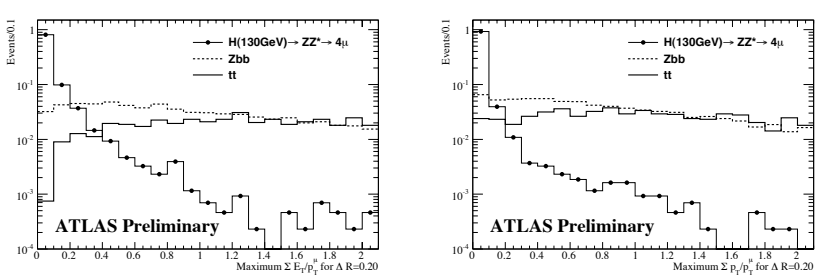

(a) (b)

Figure 5: *Normalized calorimeter (a) and track (b) isolation for the signal, $m_H = 130\, GeV$, and the main reducible backgrounds for the 4μ channel.*

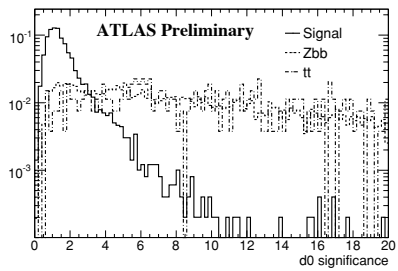

Figure 6: *Maximum impact parameter significance for the signal (m_H = 130 GeV) and reducible backgrounds in the 4μ channel.*

mass distributions, including all three topologies, for signal and background after event selection are presented in Fig. 8 for three different Higgs masses. In all three cases, the expected signal is clearly seen above the background.

The updated analysis is in its final stages, where possible improvements from the use of multivariate techniques are being studied. The estimation of the experimental backgrounds from the data is also under study, while the expected significance is treated rigorously taking into account the systematic effects. In Fig. 9 the expected significance, based on older studies [3, 7], for all the Higgs channels as a function of the Higgs mass is summarized to provide

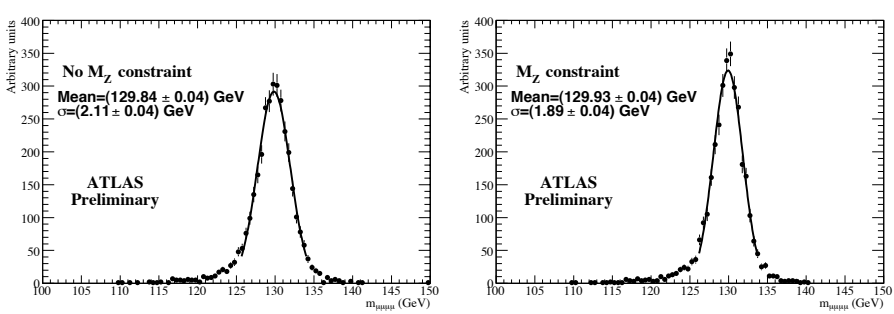

(a) (b)

Figure 7: *The reconstructed Higgs boson mass distribution in the $H \to ZZ^* \to 4\mu$ channel for $m_H = 130\,GeV$ before (a) and after (b) the Z mass constraint is applied.*

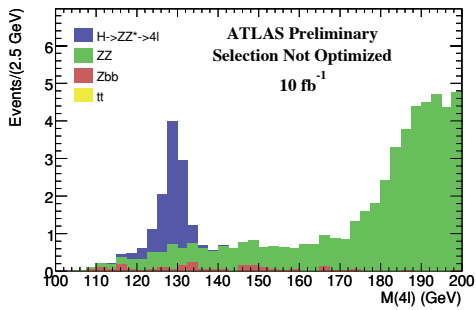

(a)

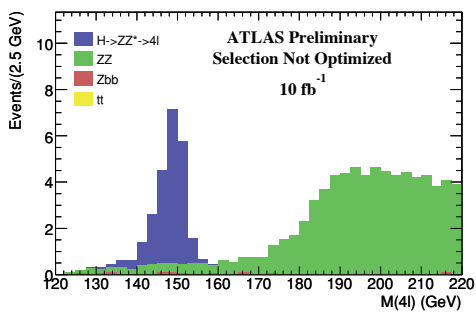

(b)

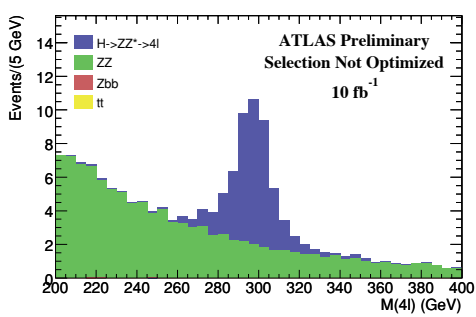

(c)

Figure 8: *Four lepton reconstructed mass distributions for the Higgs signal and backgrounds, including all three topologies, after the selection, for Higgs masses 130 GeV(a), 150 GeV(b) and 300 GeV (c).*

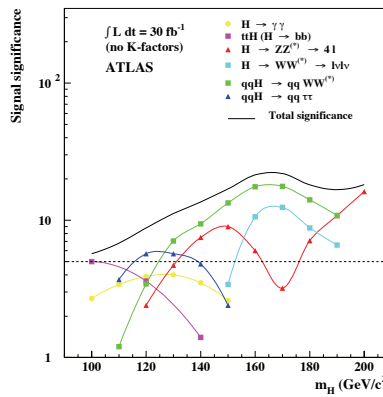

Figure 9: *ATLAS sensitivity for the discovery of the Standard Model Higgs boson for an integrated luminosity of* $30 fb^{-1}$*. The significance of the individual channels and their combination is presented as a function of the Higgs mass. No K-factors are used.* [3, 7].

some hints on the expected results. However, in this significance estimation no Next-to-Leading Order K-factors were used. Indeed, the preliminary results show that, depending on the Higgs mass, discoveries are already possible with few fb^{-1} of integrated luminosity.

6 Measurement of Higgs parameters

In the case where the Standard Model Higgs boson is discovered at the LHC, the effort will be concentrated in the measurement of its properties, both in order to understand the nature of the newly discovered particle and to test the Standard Model - which after fixing the Higgs mass can give predictions for all its properties. The $H \rightarrow ZZ^{(*)} \rightarrow 4l$ channel is one of the most promising channels for many of these measurements.

As shown in Fig. 10(a), the Higgs mass will be measured in a wide mass range to the 0.1% level with $300 fb^{-1}$ of integrated luminosity, with the main systematic uncertainty being the energy scale of the leptons. The direct measurement of the natural width of the Higgs boson is only possible for high Higgs boson masses, where an uncertainty of $\approx 8\%$ is to be expected for Higgs masses above 270 GeV, Fig. 10(b). The Higgs production rate, $\sigma \times BR$, will be measured to $\approx 10\%$, Fig. 10(c), with the ultimate precision being limited

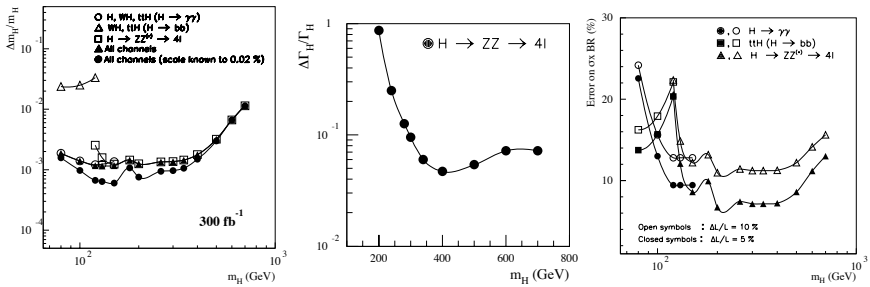

(a) (b) (c)

Figure 10: *Relative precision on the measured Higgs boson mass (a) total decay width (b) and production rate (c) as a function of the Higgs mass for* $300\, fb^{-1}$ *of integrated luminosity* [3].

by the precision of the absolute luminosity measurement at the LHC.

The spin and CP quantum numbers of the Higgs boson will be determined in the $H \to ZZ \to 4l$ channel by exploiting the correlations in the angular distributions of the leptons [8]. While, the $H \to ZZ^{(*)} \to 4l$ will be combined with other channels, like the $H \to WW^{(*)}$, to estimate ratios of Higgs couplings [9].

7 Summary

The $H \to ZZ^{(*)} \to 4l$ channel has a large discovery potential in the LHC. It is the "gold-plated" channel for Standard Model Higgs discovery in the high mass region ($M_H > 200\, GeV$) with the distinctive signature of two on-shell Z bosons decaying to leptons, while it is a very important channel in the Standard Model favored low mass region, especially during the start-up phase. If the Standard Model Higgs is discovered, then the $H \to ZZ^{(*)} \to 4l$ channel will be used to measure it properties and fully verify the Standard Model, provided there is enough integrated luminosity.

The ATLAS detector, with its excellent lepton identification and measurement capabilities, is well-suited for this analysis. The first results of the updated analysis indicate that the combination of different decay channels allows the discovery of a signal with a fb^{-1} of well understood data.

However, before being able to exctract discovery signals from LHC collisions the ATLAS collaboration will perform extensive measurements of the

main Standard Model processes in order to prove the good performance of the detector and the required understanding of the data.

8 Acknowledgements

The author would like to thank the organizers of the Rencontres de Physique de la Vallée d'Aoste for the excellent organization of this stimulating conference and the support provided through the grant for young physicists.

The support of the ATLAS Higgs working group is acknowledged and greatly appreciated. The author is particularly indebt to A. Nisati, L. Fayard, S. Paganis, S. Rosati, D. Rebuzzi, C. Kourkoumelis, D. Fassouliotis and V. Polychronakos for their useful comments during the preparation of the talk and of this manuscript.

References

1. J. Alcaraz *et al.* [LEP Collaborations], arXiv:hep-ex/0712.0929.
2. R. Barate *et al.* [LEP Working Group for Higgs boson searches], Phys. Lett. B **565** (2003) 61.
3. ATLAS Collaboration, ATLAS detector and physics performance Technical Design Report, CERN/LHCC 99-14/15 (1999).
4. U. Aglietti *et al.*, Tevatron-for-LHC Report: Higgs, FERMILAB-CONF-0-467-E-T, arXiv:hep-ph/0612172 (2006).
5. A. Djouadi, J. Kalinowski and M. Spira, Comput. Phys. Commun. **108** (1998) 56.
6. ATLAS Collaboration, The ATLAS Experiment at the CERN Large Hadron Collider, submitted to JINST.
7. S. Asai *et al.*, Eur. Phys. J. C **32S2** (2004) 19.
8. C. P. Buszello, I. Fleck, P. Marquard and J. J. van der Bij, Eur. Phys. J. C **32** (2004) 209.
9. M. Dührssen, Prospects for the measurement of Higgs boson coupling parameters in the mass range from $110 - 190\,GeV/c^2$, ATLAS note, ATLAS-PHYS-2003-030.